Fusion Engineering and Design 136 (2018) 925–930

Contents lists available at ScienceDirect

Fusion Engineering and Design

journal homepage: www.elsevier.com/locate/fusengdes

Direct numerical simulation of liquid metal free-surface turbulent flows imposed on wall-normal magnetic field

Yoshinobu Yamamoto[a,*], Tomoaki Kunugi[b]

[a] Division of Mechanical Engineering, University of Yamanashi, 4-3-11 Takeda, Kofu, 400-8511, Japan
[b] Department of Nuclear Engineering, Kyoto University C3-d2S06, Kyoto-Daigaku Katsura, Nishikyo-Ku, Kyoto, 615-8540, Japan

ARTICLE INFO

Keywords:
Liquid metal MHD
Free-surface turbulent flow
DNS
Turbulence modeling

ABSTRACT

To investigate Magneto-Hydro-Dynamics (MHD) effects on structures of turbulence near a free surface, Direct Numerical Simulations (DNS) of free surface turbulent flows imposed on a wall-normal magnetic field were conducted under the friction Reynolds number 400 with the Hartmann number 0, 10, 14, and 16. As the results, we can succeed to obtain the all information to develop and validate the RANS model such as a k-epsilon model.

Near free surface, the MHD dissipation term of the turbulent kinetic energy shows the dominant contribution, but one of the turbulent dissipation rate gives little influence for the transport process. Furthermore, the validity of the modeling of MHD effects on the free-surface proposed by Smolentsev et al., Int. J. Eng. Sci. (2002) was shown by means of the present DNS database.

1. Introduction

Free-surface turbulent flows under the magnetic forces are very often found in nuclear fusion reactor engineering fields [1–5] etc. Due to the Magnet-Hydro-Dynamic (MHD) effects, free-surface turbulent structures are modulated into the laminarization [6], as the results the turbulent heat transfer accoss the free-surface is also suppressed [7]. Therefore, to understand the free-surface tubulent structures of the liquid metal flows under magnetic fileds is of paticular importance for modeling of turbulence such as the Reynolds averaged Navier-Stokes simulation (RANS).

Free-surface turbulent flows are divided into two types of flow regimes. One is the low-Froude number flow, in which the Froude number [$Fr = U_b/(gh)^{1/2}$, where U_b is bulk mean velocity, g is gravitational acceleration, and h is flow depth] is less than 0.5. In low-Fr range, surface deformation is small, hence the free-surface can be regarded as a rigid-lid free-surface. On the other hand, in high-Fr flow ($Fr > 1.0$), free-surface normal turbulent-intensity has a tendency to increase, and surface deformation effects no longer be neglected. To understand the free-surface turbulent structures, direct numerical simulation (DNS) of a rigid-lid free-surface turbulent flow was initially conducted by Lam and Banergee [8]. Handler et al. [9] also conducted DNS of an open-channel flow and obtained turbulent statistics such as the budgets of Reynolds stress and turbulent dissipation-rate near the rigid-lid free-surface. For high-Fr flow, Yamamoto and Kunugi [10] was conducted a DNS of the free-surface turbulent flow at $Fr = 1.8$. As stated above, free-surface turbulent structures under non-MHD fields are well-understood until now.

On the other hand, in our knowledge, Satake et al. [6] only succeeded to obtained the near free surface turbulent statistics such as the budgets of turbulent kinetic energy (k) under the MHD effects. However, the budgets of turbulent dissipation rate (ε), which is the one of key factors from the viewpoints of turbulence modeling such as the low-Reynolds (Re) number k-epsilon (k-ε) model, have not yet been established. In fact, the prediction accuracy of the low-Re k-ε model is strongly depended on the modeling accuracy of the transport equation of ε in channel flows under the MHD effects [11,12].

In this study, we established the DNS database of all information to develop the low-Re k-ε model for the free-surface turbulent flows imposed on the wall-normal magnetic field, and investigated MHD effects on structures of turbulence near a free surface.

2. Overview of the DNS database

2.1. Target flow fields

The target flow is an incompressible MHD turbulent flow at a low magnetic Reynolds number.in the previous DNS study [6]. In this previous study [6], the effects of the magnetic fields for streamwise or spanwise directions on fundamental turbulent statistics are discussed. With regards to wall-normal magnetic fields, the most remarkable effects on the dissipation length scale at the free surface are appeared

* Corresponding author.
E-mail address: yamamotoy@yamanashi.ac.jp (Y. Yamamoto).

https://doi.org/10.1016/j.fusengdes.2018.04.041
Received 16 November 2017; Received in revised form 10 April 2018; Accepted 11 April 2018
Available online 25 May 2018

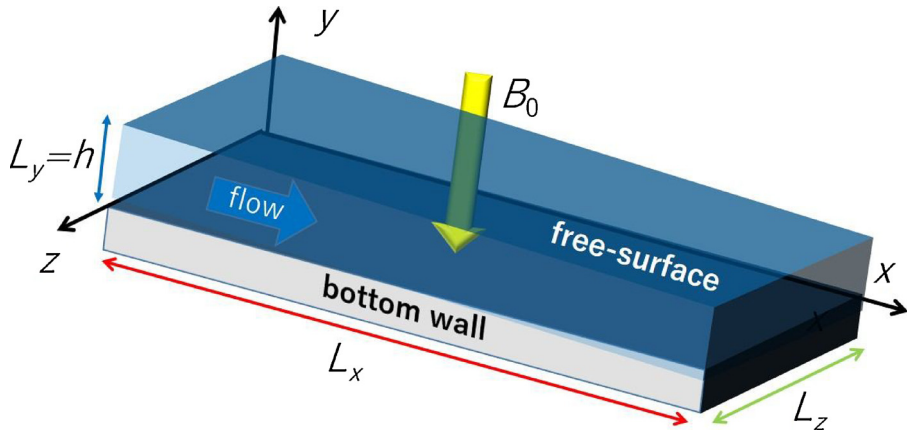

Fig. 1. Flow geometry and coordinate system.

[13]. The present flow is assumed to be a fully-developed rigid-rid open-channel flow in the presence of a wall-normal uniform magnetic field. Thermal properties of the present liquid-metal flows are used them of lithium at 500 °C. The flow geometry and coordinate system are shown in Fig. 1, where B_0 is the wall-normal uniform magnetic field, h is the flow depth, and L_x, L_y, L_z are the streamwise (x), wall-normal (y), and spanwise (z) computational lengths, respectively.

2.2. Governing equations and numerical procedures

The continuity, and the momentum equations with an electric field described using the electrical potential approach at a low–magnetic Reynolds number, were solved using a hybrid Fourier spectral method and a second-order central differencing method. To remove the aliasing errors derived from nonlinear terms, the phase-shift method was applied. The time integration methods for the governing equations were as follows: the third-order Runge–Kutta scheme was used for the convection terms, the Crank–Nicolson scheme was used for the viscous terms, and the Euler implicit scheme was used for the pressure terms. The Helmholtz equation for the viscous terms and the Poisson equations for the pressure and electrical potential were solved using a tri-diagonal matrix algorithm in Fourier space.

For the velocity fields, nonslip and free-slip condition was imposed on the bottom-wall and free surface respectively, and periodic condition was used for the stream and spanwise directions. For the electric potential, non-conducting condition was applied on the bottom-wall and the free surface, and a periodic condition was also imposed on the stream and spanwise directions. The spanwise total electric current was maintained at zero [14].

2.3. Numerical conditions

The numerical conditions for the present DNS are shown in Table 1, where the superscript + denotes the non-dimensional quantities normalized by friction velocity (u_τ) and kinematic viscosity (ν). In our computations, the friction Reynolds number, $\mathrm{Re}_\tau = u_\tau\, h/\nu$, was kept constant at 400. The Hartmann number, $\mathrm{Ha} = B_0\, h\, (\sigma/\rho\nu)^{1/2}$, where σ is the electrical conductivity and ρ is the density, was changed from 0 to 16. The bulk Reynolds numbers ($\mathrm{Re_b} = U_b h/\nu$, where U_b is the streamwise bulk velocity) were approximately 8000.

Table 1
Numerical conditions.

Reτ	Ha	domain L_x, L_y, L_z	grid number N_x, N_y, N_z	resolution Δx^+,Δy^+,Δz^+
400	0, 10, 14, 16	12.8 h, h, 6.4 h	384, 192, 384	13.3, 0.3–4.3, 6.7

Reτ = $u_\tau h/\nu$: friction Reynolds number, u_τ: friction velocity, h: flow depth, ν: kinematic viscosity, $\mathrm{Ha} = B_0 h(\sigma/\rho\nu)^{1/2}$, Hartmann number, B_0: wall-normal magnetic flux density, σ: electric conductivity, L_x (N_x, Δx), L_y (N_y, Δy), L_z (N_z, Δz): computational domain (grid number, resolution) for stream (x), vertical (y), and spanwise (z) directions, respectively.

The computations were performed on a Fujitsu FX100 and a NEC SX-ACE supercomputer systems at National Institute for Fusion Science and Tohoku University. To obtain the statistical values, the time integration was conducted during 8000 in the normalized time units based on friction velocity and kinematic viscosity for all cases.

2.4. Reynolds averaged momentum equation

The Reynolds Averaged equation of the Navier-Stokes equation in this study is written as

$$\underbrace{\frac{\partial U^+}{\partial y^+}}_{\text{viscous stress}} \underbrace{-\overline{u^+v^+}}_{\text{Reynolds stress}} + \underbrace{\frac{\mathrm{Ha}^2}{\mathrm{Re}_\tau{}^2}\int_0^{y^+}(U_b{}^+ - U^+)dy'^+}_{\text{MHD stress}} = \underbrace{1 - \frac{y^+}{\mathrm{Re}_\tau}}_{\text{total stress}}. \tag{1}$$

The total shear stress is the function of y^+ and consists of the viscous shear stress, the Reynolds stress and the magnetic stress. In k-ε model [15], Reynolds stress is related to the mean rate of strain ($\partial U/\partial y$) via a turbulent viscosity (ν_T), i.e.

$$-\overline{u^+v^+} = \nu_T{}^+\frac{\partial U^+}{\partial y^+},\quad \nu_T{}^+ = C_\mu\frac{k^{+2}}{\varepsilon^+}. \tag{2}$$

Here, $C\mu$ is a model constant and the standard value is 0.09 [15]. To obtain the Reynolds stress in right side of Eq. (2), turbulent kinetic energy (k) and turbulent dissipation rate (ε) are required.

2.5. Transport equation of turbulent kinetic energy and energy dissipation rate

The transport equations of turbulent kinetic energy (k) and turbulent dissipation rate (ε) for the fully-developed open-channel flow under the wall-normal magnetic field, are given by Eqs. (3) and (4), respectively.

$$\frac{Dk}{Dt} = \underbrace{-\overline{uv}\frac{\partial U}{\partial y}}_{P_k} + \underbrace{\frac{\partial}{\partial y}\left(-\frac{\overline{u_i u_i v}}{2}\right)}_{T_k} + \underbrace{\nu\frac{\partial^2 k}{\partial y^2}}_{D_k} + \underbrace{\frac{\partial}{\partial y}\left(-\frac{\overline{pv}}{\rho}\right)}_{\Pi_k} - \underbrace{\nu\overline{\left(\frac{\partial u_i}{\partial x_j}\right)^2}}_{\varepsilon} + \underbrace{\frac{\sigma B_0}{\rho}\left(-u\overline{\frac{\partial\phi}{\partial z}} + w\overline{\frac{\partial\phi}{\partial x}}\right)}_{S_k^{M1}} \underbrace{-\frac{\sigma B_0^2}{\rho}(\overline{u^2} + \overline{w^2})}_{S_k^{M2}}, \tag{3}$$

$$\frac{D\varepsilon}{Dt} = \underbrace{-2\nu\overline{\frac{\partial u}{\partial x_i}\frac{\partial v}{\partial x_i}\frac{\partial U}{\partial y}}}_{P_\varepsilon^1} \underbrace{-2\nu\overline{\frac{\partial u_i}{\partial x}\frac{\partial u_i}{\partial y}\frac{\partial U}{\partial y}}}_{P_\varepsilon^2} \underbrace{-2\nu\overline{\frac{\partial u}{\partial y}\frac{\partial^2 U}{\partial y^2}}}_{P_\varepsilon^3} \underbrace{-2\nu\overline{\frac{\partial u_i}{\partial x_j}\frac{\partial u_i}{\partial x_k}\frac{\partial u_k}{\partial x_j}}}_{P_\varepsilon^4}$$
$$+\underbrace{\frac{\partial}{\partial y}\left(-\nu\overline{\frac{\partial u_i}{\partial x_j}\frac{\partial u_i}{\partial x_j}v}\right)}_{T_\varepsilon} + \underbrace{\frac{\partial}{\partial y}\left(-2\nu\overline{\frac{1}{\rho}\frac{\partial p}{\partial x_i}\frac{\partial v}{\partial x_i}}\right)}_{\Pi_\varepsilon}$$
$$+\underbrace{\nu\frac{\partial^2\varepsilon}{\partial y^2}}_{D_\varepsilon} \underbrace{-2\nu^2\overline{\frac{\partial^2 u_i}{\partial x_j\partial x_k}\frac{\partial^2 u_i}{\partial x_j\partial x_k}}}_{\gamma}$$
$$+\underbrace{2\frac{\nu\sigma B_0}{\rho}\left(-\overline{\frac{\partial u}{\partial x_j}\frac{\partial^2\phi}{\partial x_j\partial z}} + \overline{\frac{\partial w}{\partial x_j}\frac{\partial^2\phi}{\partial x_j\partial x}}\right)}_{S_\varepsilon^{M1}} \underbrace{-2\frac{\nu\sigma B_0^2}{\rho}\left[\overline{\left(\frac{\partial u}{\partial x_j}\right)^2} + \overline{\left(\frac{\partial w}{\partial x_j}\right)^2}\right]}_{S_\varepsilon^{M2}}$$
$$= 0 \tag{4}$$

Here, D/Dt is the substantial derivative, u_i and x_i are the streamwise ($u_1 = u$, $x_1 = x$), vertical ($u_2 = v$, $x_2 = y$,), and spanwise ($u_3 = w$, $x_3 = z$,) turbulent velocities and directions, respectively. U is the streamwise mean velocity, p is the pressure, ϕ is the electric potential, and over bar ($\overline{\ }$) denotes a time average.

The transport Eq. (3) of the turbulent kinetic energy is classified into three terms for types of their contributions; the production term (P_k), the diffusion terms comprised of the turbulent diffusion (T_k), the viscous diffusion (D_k) and the pressure diffusion (Π_k), and the dissipation terms comprised of the viscous dissipation (ε) and the magnetic dissipation (S_k^{M1}, S_k^{M2}).

The transport Eq. (4) of the turbulent energy dissipation rate is also classified into three terms. The production terms comprise the mixed production (P_ε^1), the production by mean velocity (P_ε^2), the gradient production (P_ε^3), and the turbulent production (P_ε^4). The diffusion terms comprise the turbulent diffusion (T_ε), the pressure diffusion (Π_ε), and the viscous diffusion (D_ε). The destruction (dissipation) terms comprise the viscous destruction rate (γ) and the magnetic destruction terms (S_ε^{M1}, S_ε^{M2}). Two types of MHD terms both in Eqs. (3) and (4) were considered as one dissipative source term. In short, the Lorentz force always acted as the dissipative contribution to the turbulent energy dissipation rate [16]. The main objective of the present study is to obtain the DNS database in Eqs. (1)–(4) as the reference data in the turbulence modeling.

3. Results and discussion

3.1. MHD effects of mean momentum equation

Fig. 2 show the Reynolds Averaged equation of the Navier-Stokes Eq. (1) for Ha = 0, 14, and 16, respectively. With increasing Hartmann number, the magnetic stress becomes larger which is known well as the MHD pressure loss and the Reynolds stress is reduced. In case of Ha = 14, the Reynolds stress and the magnetic stress show the same level, and the magnetic stress exceeds the Reynolds stress over all wall-normal heights in case of Ha = 16. Accordingly, the reduction of the Reynolds shear stress changes the turbulent flow into the laminar flow in case of Ha ≥ 16.

The model constant ($C\mu$) of the turbulent viscosity is evaluated in at the log-region of the mean velocity profile as [17]

$$C_\mu^2 = \frac{-\overline{uv}}{k}. \tag{5}$$

The Hartman number effect on Eq. (5) is shown in Fig. 3. C_μ shows the almost same value as the standard value 0.09 except for Ha = 16.

The dissipation length (l) can be estimated as,

$$l \approx \frac{k^{3/2}}{\varepsilon}. \tag{6}$$

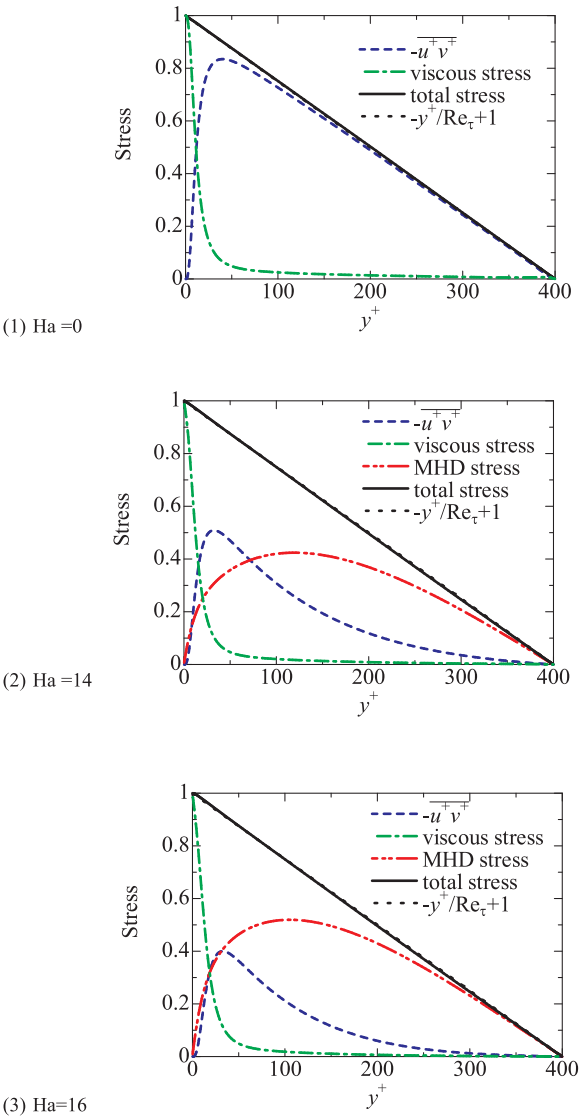

Fig. 2. The balance of the mean momentum equation.

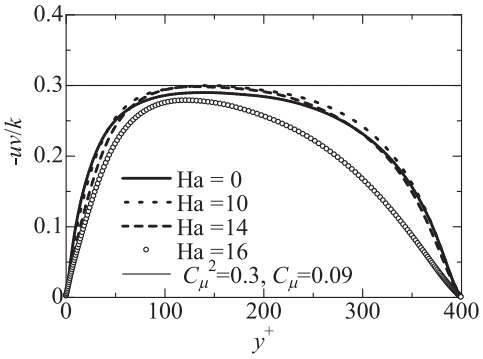

Fig. 3. Ha effects of model constant: C_μ.

Fig. 4 shows the Hartmann number effects on the dissipation length scale at the free surface normalized by the one of Ha = 0. The only k-ε model under the free surface MHD flows was proposed by Smolentsev et al. [13]. In this model [13], MHD effects on the free surface turbulent statistics are considered as the decrease of the dissipation length scale (l) at the free surface as shown in Fig. 4. The present results for Ha = 10 and 14 show good agreement with the model [13]. The changes of the model constant and the dissipation length at the free surface in case of

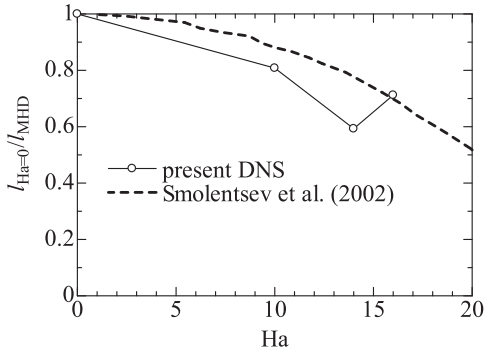

Fig. 4. Ha effects of the dissipation length scale at the free-surface.

Ha = 16 are caused from the remarkable laminarization as shown in Fig. 2(3).

3.2. MHD effects on the transport of turbulent kinetic energy and dissipation rate

Near free surface, the budgets of the turbulent kinetic energy (k) in cases of Ha = 0 and 16 are shown in Fig. 5. All terms in Eq. (3) were normalized using u_τ^4/ν. In case of Ha = 0, near free surface turbulent kinetic energy was supplied through the pressure diffusion (Π_k) and the turbulent diffusion (T_k), and was lost through the viscous dissipation (ε) and the viscous diffusion (D_k). In case of Ha = 16, turbulent kinetic energy is gained through the pressure diffusion (Π_k) and is lost through

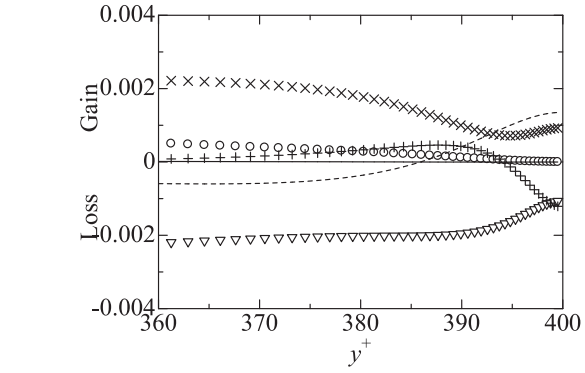

(1) Ha =0

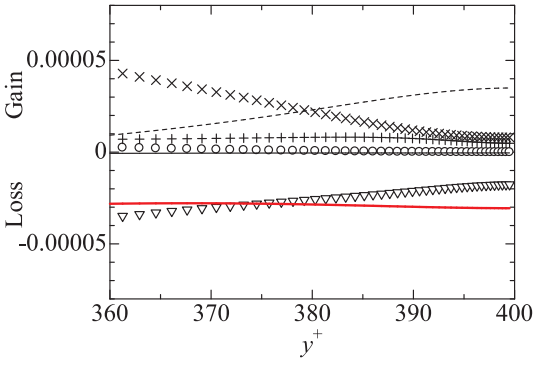

(2) Ha=16

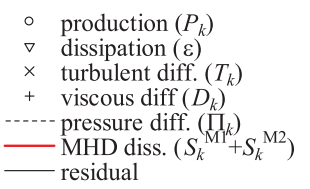

Fig. 5. Ha effects on budget of the turbulent kinetic energy, near free-surface.

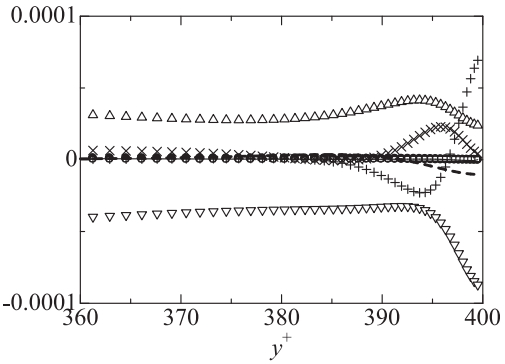

(1) Ha =0

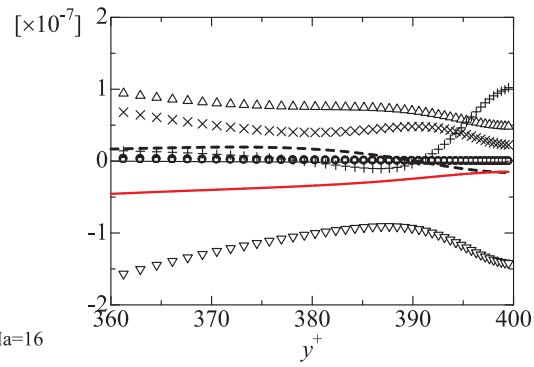

(2) Ha=16

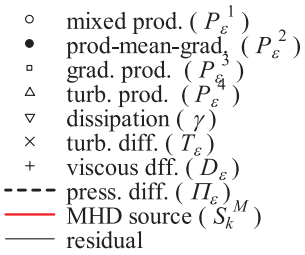

Fig. 6. Ha effects on budget of the turbulent dissipation rate, near free surface.

the viscous dissipation (ε) and the magnetic dissipation ($S_k^{M1} + S_k^{M2}$). Since the pressure diffusion term (Π_k) is usually ignored or implicitly included in the T_k term, the underestimation of k is concerned near free surface. Besides, the quantitative prediction of the MHD effects is required because the magnetic dissipation term plays the primary role at the vicinity of the free surface.

Fig. 6 shows the budgets of the turbulent energy dissipation (ε) rate in cases of Ha = 0 and 16. All terms in Eq. (4) were normalized using u_τ^6/ν^2. In case of Ha = 0, the supply from the viscous diffusion (D_ε) is dominant, and balances with the loss from the viscous destruction rate (γ). It is surprising that the almost same transport process of ε near free surface, is confirmed in case of Ha = 16. The contribution of the magnetic dissipation is relatively small, but the turbulent production (P_ε^4) has the significant value both in cases of Ha = 0 and 16. Therefore, the generally modeling used $P_\varepsilon^4 - \gamma$ in ε - equation [18] can be useful in the MHD free surface flows. Finally, the mechanism of turbulent energy and dissipation rate transport near the free surface is summarized in Fig. 7.

3.3. A priori test of MHD dissipative terms

The MHD dissipative models in k- and ε-equations are proposed by Ji & Gradner [19], Kenjeres & Hanjalic [16], and Smolentsev et al. [13]. The model proposed by Smolentsev et al. [13] only has been studied the applicability for the free surface. This model expression is as follows;

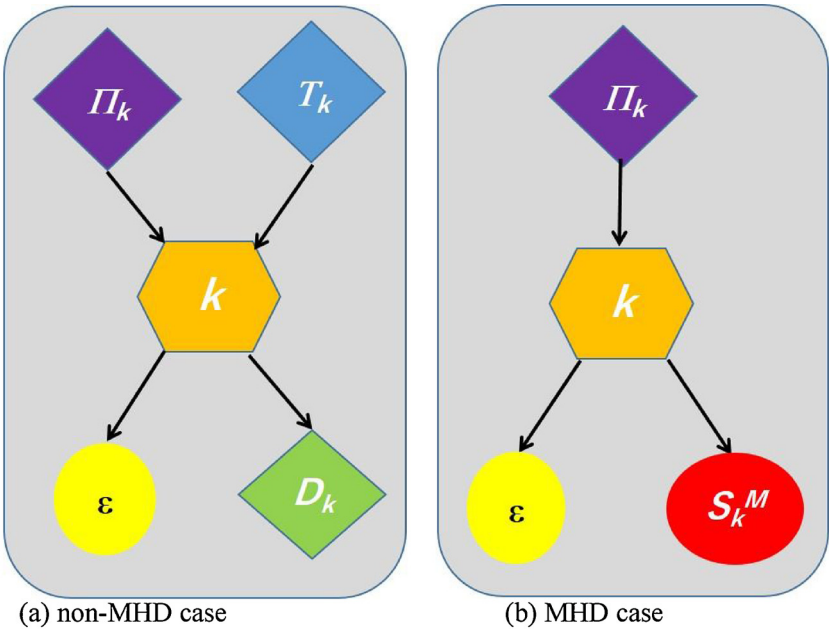

Fig. 7. The mechanism of turbulent energy and dissipation transport, near the free surface.

$$S_k^M = -C_3\frac{\sigma}{\rho}B_0^2 k,\ C_3 = 1.9\exp(-1.0N),\ N = \frac{\sigma B_0^2 2h}{\rho U_b}, \tag{7}$$

$$S_\varepsilon^M = -C_4\frac{\sigma}{\rho}B_0^2 \varepsilon,\ C_4 = 1.9\exp(-2.0N),\ N = \frac{\sigma B_0^2 2h}{\rho U_b}. \tag{8}$$

Fig. 8 shows the a priori test of the MHD dissipative model. The model by Smolentsev et al. [13] can predict DNS results quantitatively.

4. Conclusions

In this study, we succeeded in establishing DNS database of turbulent free surface flows imposed on a wall-normal uniform magnetic field. Near free surface, the importance of modeling in the pressure diffusion and the MHD dissipation terms of the turbulent kinetic energy is revealed on a k-ε model. Although the dissipation length shows the decreasing tendency with increasing of Ha, the transport process of the turbulent dissipation rate near the free surface has the almost same mechanism with or without MHD effects. Present DNS results show the

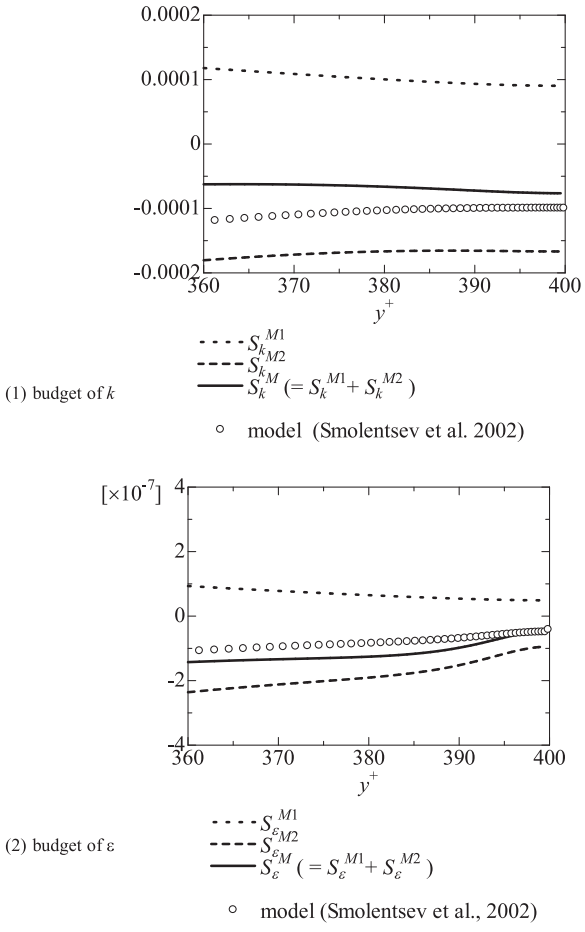

Fig. 8. A priori testing of MHD source terms in k and ε-equation, near free surface.

validity of the modeling of MHD effects on the free surface proposed by Smolentsev et al., Int. J. Eng. Sci. (2002).

Acknowledgments

This work was supported by JSPS KAKENHI Grant Number 15K05790, and this research used computational resources of "Joint Usage/Research Center for Interdisciplinary Large-scale Information Infrastructures" in Japan (Project IDs: jh160045-MDJ and jh170043), and Plasma simulator at National Institute for Fusion Science (NIFS).

References

[1] M.A. Abdou, A. team, Exploring novel high power density concepts for attractive fusion systems, Fusion Eng. Des. 45 (2) (1999) 145–167.
[2] N.B. Morley, S. Smolentsev, R. Munipalli, M.J. Ni, D. Gao, M. Abdou, Progress on the modeling of liquid metal, free surface, MHD flows for fusion liquid walls, Fusion Eng. Des. 72 (1) (2004) 3–34.
[3] K. Kusumi, T. Kunugi, T. Yokomine, Z. Kawara, J.A. Hinojosa, E. Kolemen, E. Gilson, Study on thermal mixing of liquid–metal free-surface flow by obstacles installed at the bottom of a channel, Fusion Eng. Des. 109 (2016) 1193–1198.
[4] T. Okita, J. Morioka, E. Hoashi, H. Okuno, H. Horiike, Study on suppression of free surface fluctuation of liquid Li jet by magnetic field, Fusion Eng. Des. 124 (2017) 975–979.
[5] S. Smolentsev, M. Abdou, C. Courtessole, G. Pulugundla, F.C. Li, N. Morley, T. Rhodes, Review of recent mhd activities for liquid metal blankets in the us, Magnetohydrodynamics 53 (2) (2017).
[6] S. Stake, T. Kunugi, S. Somlentsev, Advances in direct numerical simulation for MHD modeling of free surface flows, Fusion Eng. Des. 61–62 (2002) 95–102.
[7] A.Y. Ying, N. Morley, S. Smolentsev, K. Gulec, P. Fogarty, Free surface heat transfer and innovative designs for thin and thick liquid walls, Fusion Eng. Des. 49 (2000) 397–406.
[8] K. Lam, S. Banerjee, On the condition of streak formation in a bounded turbulent flow, Phys. Fluids A 4 (2) (1992) 306–320.
[9] R. Handler, T.F. Swean, R.I. Leighton, J.D. Swearingen, Length scales and the energy balance for turbulence near a free surface, AIAA J. 31 (11) (1993) 1998–2007.
[10] Y. Yamamoto, T. Kunugi, Direct numerical simulation of a high-froude-number turbulent open-channel flow, Phys. Fluids 23 (12) (2011) 125108.
[11] Y. Yamamoto, T. Kunugi, MHD effects on turbulent dissipation process in channel flows with an imposed wall-normal magnetic field, Fusion Eng. Des. 109 (2016) 1137–1142.
[12] Y. Yamamoto, N. Osawa, T. Kunugi, A new RANS model in turbulent channel flow imposed wall-normal magnetic field with heat transfer, Fusion Sci. Technol. 72 (4) (2017) 601–608.
[13] S. Smolentsev, M. Abdou, N. Morley, A. Ying, T. Kunugi, Application of the K–ε model to open channel flows in a magnetic field, Int. J. Eng. Sci. 40 (6) (2002) 693–711.
[14] Y. Shimomura, Large eddy simulation of magnetohydrodynamic turbulent channel flows under a uniform magnetic field, Phys. Fluids A 3 (12) (1991) 3098–3106.
[15] W.P. Jones, B. Launder, The prediction of laminarization with a two-equation model of turbulence, Int. J. Heat Mass Transfer 15 (2) (1972) 301–314.
[16] S. Kenjereš, K. Hanjalić, On the implementation of effects of Lorentz force in turbulence closure models, Int. J. Heat Fluid Flow 21 (3) (2000) 329–337.
[17] W. Rodi, N.N. Mansour, Low Reynolds number k—ε modelling with the aid of direct simulation data, J. Fluid Mech. 250 (1993) 509–529.
[18] B.E. Launder, G.J. Reece, W. Rodi, Progress in the development of a Reynolds-stress turbulence closure, J. Fluid Mech. 68 (3) (1975) 537–566.
[19] H.C. Ji, R.A. Gardner, Numerical analysis of turbulent pipe flow in a transverse magnetic field, Int. J. Heat Mass Transfer 40 (8) (1997) 1839–1851.